Research Article | Vol. 27, No. 21 / 14 October 2019 / Optics Express 29491
Optics EXPRESS

Impact of deuteration on the ultrafast nonlinear optical response of toluene and nitrobenzene

CHRISTIAN KARRAS,[1] MARIO CHEMNITZ,[1] RAINER HEINTZMANN,[1,2] AND MARKUS A. SCHMIDT[1,3,4,*]

[1]Leibniz Institute of Photonic Technology, Albert-Einstein-Straße 9, 07745 Jena, Germany
[2]Institute of Physical Chemistry and Abbe Center of Photonics, Friedrich-Schiller-University, Helmholtzweg 4, 07743 Jena, Germany
[3]Abbe Center of Photonic and Faculty of Physics, Friedrich-Schiller-University Jena, Max-Wien-Platz 1, Jena 07743, Germany
[4]Otto Schott Institute of Material Research, Fraunhoferstr. 6, 07743 Jena, Germany
[*]markus-alexander.schmidt@uni-jena.de

Abstract: Nonlinear pulse propagation inside highly nonlinear media requires accurate knowledge on the temporal response function of the materials used particular in the case of liquids. Here we study the impact of deuteration on the ultrafast dynamics of toluene and nitrobenzene via all optical Kerr gating, showing substantially different electronic and molecular contributions, which was quantified by fitting a multichannel decay model to the data points. Specifically we found that deuteration imposes the time-integrated nonlinearities to reduce particular for toluene which could be caused by both reduced electronic hyperpolarizabilities as well as weaker intermolecular interactions. The results achieved reveal that deuterated organic solvents represent promising materials for infrared photonics since they offer extended infrared transmission compared to their non-deuterated counterparts while maintained strong nonlinear responses.

© 2019 Optical Society of America under the terms of the OSA Open Access Publishing Agreement

1. Introduction

Tailoring the nonlinear interaction of light and matter inside optical fibers has enabled novel devices such as light sources with customized properties [1,2] or sophisticated applications in, e.g. telecommunications [3]. Many fiber devices used consist of silica materials, which can show limited performance due to restricted transmission windows and an overall small nonlinear refractive index (Δn) [4,5]. Non-silica based glass materials may represent interesting alternatives [6–10], yet difficulties in fiber fabrication, high optical loss and undefined dispersion profiles have prevented the wide-spread use of such materials for nonlinear photonics. An inherent drawback of all-glass fibers is the solid nature of the materials involved, making it difficult to fine-tune fiber properties after implementation, which can lead to severe consequences with regard to dispersion tuning.

An innovative solution to the aforementioned issues mentioned are liquid-core fibers representing a new and promising class of hybrid fibers for nonlinear applications [11–14] due to precise and real-time dispersion tuning opportunities [14] and substantially larger values of Δn [15], with the latter originating from an electronic as well as molecular contributions. Recent comprehensive studies aiming for characterizing the nonlinear properties of different solvents were performed in unprecedented detail [16,17], providing a base for the photonics community to explore entirely new nonlinear operation regimes arising from the unique non-instantaneous nonlinear dynamics of liquids [18] . It is important to note that due to its outstanding properties (e.g., high nonlinearity [19,20] and high damage threshold [21]) carbon disulfide (CS_2) has been established as the standard liquid for nonlinear experiments [22,23] while it is less applicable for applications that require biocompatibility or mixing with polar solvents or dyes.

#368873 https://doi.org/10.1364/OE.27.029491
Journal © 2019 Received 30 May 2019; revised 5 Sep 2019; accepted 6 Sep 2019; published 30 Sep 2019

Optics EXPRESS

Here, organic liquids represent promising alternatives while strong CH-overtone absorption limits their operation domain to wavelength <1 μm. This limitation excludes a large set of standard laser sources (e.g., Nd:YAG or Er:glass) from being employed in connection with liquid-core fibers that include organic materials. This is of particular disadvantage in case of benzene derivates, such as toluene, which exhibits high work-safe exposure limits (i.e., can be treated as low-hazard liquid), or nitrobenzene, which possesses a similarly strong molecular nonlinearity as CS_2 [16]. Recent experiments have shown that using the corresponding deuterated counterparts imposes the absorption bands to substantially shift to longer wavelengths as a result of the increasing effective mass of the respective molecular oscillator, considerably extending transmission windows towards longer wavelengths [24]. Note that the optical loss of deuterated nitrobenzene is below 1dB/cm for almost all wavelengths up to 2.1 μm, while the non-deuterated derivate exceeds this limit already at 1.3 μm. The impact of deuteration on the temporal nonlinear dynamics of solvents, however, has not yet been investigated. In particular, it has not been revealed if the various nonlinear processes observed in hydrogen-based liquids are still present in their deuterated counterparts and whether the corresponding mathematical models used to describe the temporal dynamics can still be applied.

In the present work, the impact of deuteration on the temporal nonlinear response of organic solvents is addressed from the experimental perspective by measuring the ultrafast nonlinear response function time-resolved using optical Kerr gating (OKG). By performing a series of pump-probe measurements on two example solvents (toluene and nitrobenzene), we show that deuteration modifies the temporal response considerably, while the well-established mathematical models still apply. Fitting these models to the data shows that the instantaneous electronic part, as well as an ultrafast component of Δn related to intermolecular interactions, are reduced for deuterated compared to non-deuterated specimen.

2. Liquids used

Due to availability in high quantities and very high purity we choose toluene/toluene-D8 (99.5 mol% purity, 99.6 mol% purity) and nitrobenzene /nitrobenzene-D5 (99 mol% purity/99.5 mol% purity) as example liquids. We also measure the nonlinear response of CS_2 (SigmaAldrich, 99.9 mol% purity), whose nonlinear properties are well documented in literature in order to characterize the setup and verify its operation [19,22].

3. Experimental

The OKG setup operates in the pump-probe configuration (Fig. 1) as follows: ultrashort laser pulses (pump pulses, τ_{pu} = (60 ± 5) fs (FWHM), Coherent Legend Elite, central wavelength λ_{pu} = 800 nm) were focused into the respective liquid ($1/e^2$-radius w_{pu} = (27 ± 1) μm) in order to induce the nonlinear refractive index modulation. The liquids themselves were located in quartz glass cuvettes of thickness d = 1 mm (wall thickness: 1 mm). The pump pulse energy inside the liquid amounted to E_{pu} = (1800 ± 20) nJ (Toluene) or E_{pu} = (960 ± 10) nJ (Nitrobenzene). A second pulse was generated by an optical parametric amplifier seeded by a fraction of the pump pulse (Coherent Opera Solo, τ_{pr} = (60 ± 5) fs, λ_{pr} = 725 nm, w_{pr} = (16 ± 0.5) μm, pulse energy E_{pu}<10 nJ) and served as probe.

The small spectral distance between pump and probe pulse ensured that the group velocity mismatch (GVM) of the two pulses is as small as possible within experimental circumstances thus to avoid coherent effects in the signals. The GVM was estimated to amount to 41 fs/mm in case of Nitrobenzene and 27 fs/mm for Toluene (group indices were taken from [25]). By using a delay stage (Fig. 1) the two pulses could be mutually delayed between -2 ps (probe before pump) and +5 ps. Both pulses were linearly polarized under a relative angle of 45°. After passing the sample and an analyzer the probe pulse energy was measured using an Ophir PD10 detector as a function of the delay time t_D between pump and probe pulse. The transmission direction

Optics EXPRESS

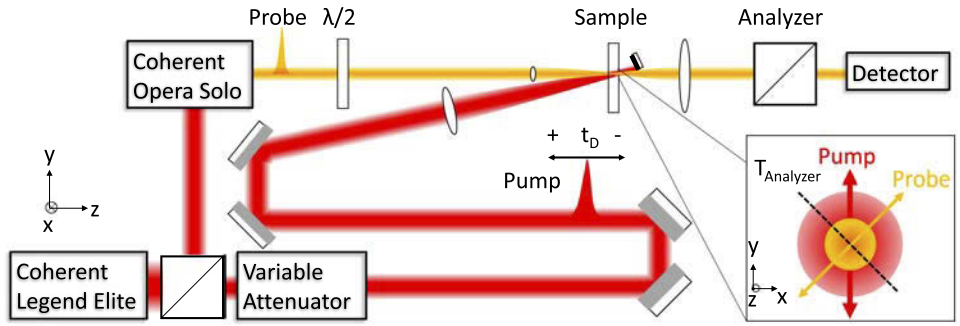

Fig. 1. Experimental setup of the ultrafast optical Kerr gate. Red: pump beam ($\tau_{pu} = 60 \pm 5$ fs, $\lambda_{pu} = 800$ nm, E_{pu} variable), yellow: probe beam ($\tau_{pr} = 60 \pm 5$ fs, $\lambda_{pr} = 725$ nm, E_{pu}<10 nJ), inset: cross section of the pump (red, $w_{pu} = 27$ μm) and the probe pulse (yellow, $w_{pr} = 16$ μm) within the sample, with the arrows indicating the respective polarization direction as well as the transmission direction of the analyzer ($T_{Analyzer}$, dashed line).

of the analyzer was perpendicular to the polarization of the incident probe, thus the nonlinear polarization rotation of the probe beam served as gate signal to reveal the nonlinear dynamics of the respective liquid.

4. Modeling

Assuming the laser pulses to be of Gaussian shape in both temporal and spatial domains the transmission of the OKG is given by the convolution:

$$T_{OKG}(t_D) = \left[\frac{4\sqrt{\ln 2}}{\sqrt{\pi}} e^{-\left(2\sqrt{\ln 2}\frac{t_D}{\tau_{pr}}\right)^2}\right] \otimes R(t_D) \tag{1}$$

with $R(t_D)$ being the apparatus function of the OKG which is computed by (c.f. appendix):

$$R(t_D) = \sum_{k=1}^{\infty} \frac{(-1)^{k-1}}{(2k)!} \frac{1}{4 + 8k w_{pr}^2/w_{pu}^2} \left(\left[\frac{8\sqrt{\ln 2}}{\sqrt{\pi}} \frac{E_{pu} d}{w_{pu}^2 \tau_p u \lambda_{pr}} e^{-\left(2\sqrt{\ln 2}\frac{t_D}{\tau_{pu}}\right)^2}\right] \otimes \Delta n(t_D)\right)^{2k} \tag{2}$$

Here the sum was computed up to $k_{max} = 10$. $\Delta n(t_D) = \sum \alpha_m n_{2,m}, r_m(t_D)$ is the time dependent nonlinear refractive index, imposed by the pump pulse and being composed of four model terms of which each represents a different physical phenomenon [16,22]: An instantaneous electronic contribution representing the electronic ($\chi^{(3)}$) response of the index modification as well as three other terms that describe the molecular processes. The molecular terms comprise collision and diffusive reorientation of the molecules as well as a coherent motion of the molecules due to the intermolecular potentials (libration) [22,26,27]. The latter was modeled to be inhomogeneously broadened as different molecules experience different local environments, which is in accordance to [22,28,29]. Each contribution consists of its individual strength ($n_{2,m}$), temporal characteristics ($r_m(t_D)$) and polarization dependency due to the field-induced index ellipsoid (α_m, details are given in Table 1) [22,30]. For the two example solvents the central frequency and spectral width of the libration were assumed to be $\omega_0 = (11 \pm 2)$ ps^{-1} and $\sigma = (8 \pm 4)$ ps^{-1} for Toluene and $\omega_0 = (7 \pm 3)$ and $\sigma = (5 \pm 2)$ ps^{-1} for Nitrobenzene, respectively [16].

Note that if the GVM is small only a broadening of the measured pulse compared to the real pulse in a pump-probe experiment is obtained [31]. In case of Toluene and CS_2 this broadening was below the uncertainty of the pulse duration and hence was neglected in the model. In case of Nitrobenzene, however, this broadening caused an effective pulse length of 68 fs, which was

Optics EXPRESS

Table 1. Temporal characteristics and polarization related factors of the different components of the nonlinear response function (δ: delta distribution, Θ: Heaviside function, θ: mutual polarization angle between pump and probe, ω_0: central libration frequency, σ: spectral width of libration, $\tau_{r;f,m}$: rise and fall times, C_m: normalization factors ($\int_{-\infty}^{+\infty} r_m(t)dt = 1$ for the individual components) [16,22].

Comp.	Temporal model	Polarization factor ($\theta = \pi/4$)
Elec.	$r_e(t) = 2\delta(t)$	$\alpha_e = \cos\theta^2 + \frac{1}{3}\sin\theta^2 = \frac{2}{3}$
Coll.	$r_c(t) = C_c\left(1 - e^{-\frac{t}{\tau_{r,c}}}\right)e^{-\frac{t}{\tau_{f,c}}}\Theta(t)$	$\alpha_c = \cos\theta^2 + \frac{1}{3}\sin\theta^2 = \frac{2}{3}$
Libr.	$r_l(t) = C_l e^{-\frac{t}{\tau_{f,d}}}\Theta(t)\int_0^\infty \frac{\sin\omega t}{\omega} g(\omega)d\omega$ with $g(\omega) = e^{-\frac{(\omega-\omega_0)^2}{2\sigma^2}} - e^{-\frac{(\omega+\omega_0)^2}{2\sigma^2}}$	$\alpha_l = \cos\theta^2 - \frac{1}{2}\sin\theta^2 = \frac{1}{4}$
Diff.	$r_d(t) = C_d\left(1 - e^{-\frac{t}{\tau_{r,d}}}\right)e^{-\frac{t}{\tau_{f,d}}}\Theta(t)$	$\alpha_d = \cos\theta^2 - \frac{1}{2}\sin\theta^2 = \frac{1}{4}$

included into the fitting procedure. Furthermore, no significant spectral broadening due to self- or cross-phase modulation was observed for either the pump or the probe pulse.

The model (1) was fitted to the data points by minimizing their least square difference. The strengths $n_{2,m}$ as well as the rise and fall times $\tau_{r;f,m}$ served as fitting parameters and the values, given in [16] as parameter initialization. Note that suppressing individual contributions in the model (by manually setting their strength $n_{2,m}$ to zero) did not lead to satisfying fitting results. The accuracy of the determined parameters has been retrieved from the fitting procedure.

5. Validation of the model

In order to validate the model the cuvette was filled with CS_2 and the transmission of the OKG was recorded as function of time for different pump pulse energies. Furthermore the transmission was computed using Eq. (1) and the parameters given in [16,19,22] (summarized in Table 2.). The measured (Fig. 2, dotted) and computed Fig. 2, lines) values agree very well, confirming the validity of the OKG approach. Slight deviations between simulated and measured results, such as the absence of the distinct trailing peak in the data points might be attributed to the uncertainty of the parameters used (c.f. Table 1. in [19]).

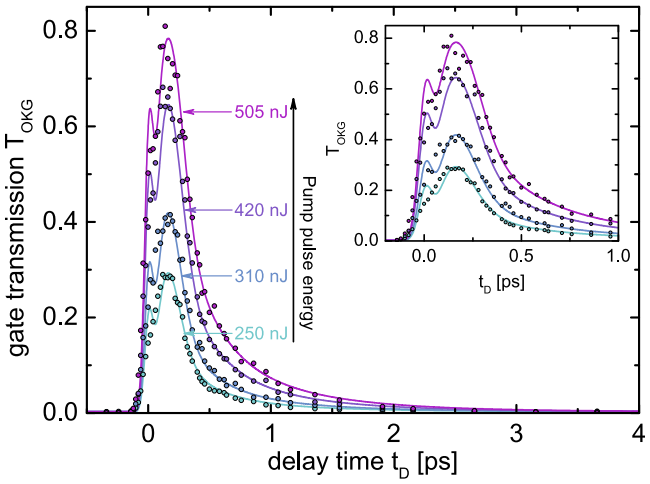

Fig. 2. CS_2 transmission of the optical Kerr gate at different pulse energies: Dots: measured values, Solid lines: Computed transmission using the model parameters from [16,19,22] and the model (1)

Optics EXPRESS

Table 2. Model parameters used for computing the time dependent OKG transmission of CS_2 at different pump pulse intensities. The values were taken from [16,19,22]

	n_2 [10^{-19} m^2/W]	τ_r [ps]	τ_f [ps]	ω_0 [ps^{-1}]	σ [ps^{-1}]
Electronic	1.5	-	-	-	-
Collision	1.0	0.15	0.14	-	-
Libration	7.6	-	0.45	-	-
Diffusion	18	0.15	1.61	8.5	5

6. Results and discussion

The parameters obtained from the fit in case of the non-deuterated specimen agree with those presented in [16] (Figs. 3(a) and 3(b), blue curves and Table 3). Using the deuterated specimen the OKG transmission is reduced for both solvents, Toluene as well as Nitrobenzene at short (t_D = ±100 fs) and intermediate (100 fs <t_D<250 fs) delay times (Figs. 3(a) and 3(b), red curves). The dominant contribution to the nonlinear refractive index on very short time scales is the intramolecular instantaneous electronic response $n_{2,elec}$. Our measurements indicate that $n_{2,elec}$ of the deuterated solvents is smaller compared to the corresponding non-deuterated specimen (Toluene 5 %, Nitrobenzene 10 %, c.f. Figures 3(a) and 3(b), dotted lines, Table 3). This is in qualitative agreement with previous experimental findings [32] and theoretical modeling [33] and might be rationalized by the larger binding energy of the C-D compared to the C-H bond [34], which imposes the electron ensemble to respond more harmonically.

Table 3. Fit parameters for the different components of the nonlinear response function for the non-deuterated (N-D, the values from Ref. [16] in parentheses) and deuterated (D) versions of toluene and nitrobenzene. Values of τ_r and τ_f in ps and values of n_2 in 10^{-19} m^2/W

		Toluene			Nitrobenzene		
		N-D		D	N-D		D
Elec.	n_2	0.42±0.02	(0.6)	0.40±0.02	0.6±0.05	(0.6)	0.54±0.05
Coll.	n_2	0.15±0.02	(0.12)	0.44±0.04	0.42±0.04	(0.35)	0.65±0.05
	τ_r	0.1(5) ± 0.1	(0.25)	0.5±0.15	0.1±0.05	(0.2)	<0.05
	τ_f	0.1±0.05	(0.2)	0.10±0.02	0.06±0.02	(0.1)	0.3±0.1
Libr.	n_2	0.96±0.05	(1.2)	0.13±0.05	1.9±0.2	(1.7)	1.3±0.15
	τ_f	0.36 ± 0.07	(0.35)	0.46 ± 0.25	0.3(5) ± 0.1	(0.4)	0.15 ± 0.05
Diff.	n_2	2.8±0.2	(3)	2.5±0.2	5.4±0.5	(5)	5.1±0.5
	τ_r	0.18±0.07	(0.25)	0.3±0.1	<0.1	(0.1)	<0.1
	τ_f	2.2±0.5	(2.1)	2.3±0.5	3.4±0.5	(3.5)	3.5±0.5
$\Delta n = \sum n_2$		4.3±0.3		3.5±0.3	8.3±0.8		7.6±0.8

The reduction of the OKG transmission for delay times between 100 fs <t_D<250 fs is majorly attributed to a change of the nonlinear refractive index contributions related to fast molecular interactions, i.e. collision and libration.

The present fitting results indicate that deuteration increases the collisional contribution to the nonlinear refractive index in case of toluene, but decreases it for nitrobenzene. The related summed time constant (τ_r + τ_f) increases in both cases. The libration related component on the other hand is reducing for both molecules after deuteration, with this effect being much stronger for toluene (c.f. Figures 3(a) and 3(b) and Table 3).

The collisional contribution to the refractive index modification arises from variations of the molecular polarizability induced by dipole interactions with neighboring molecules [22,35]. This

Optics EXPRESS

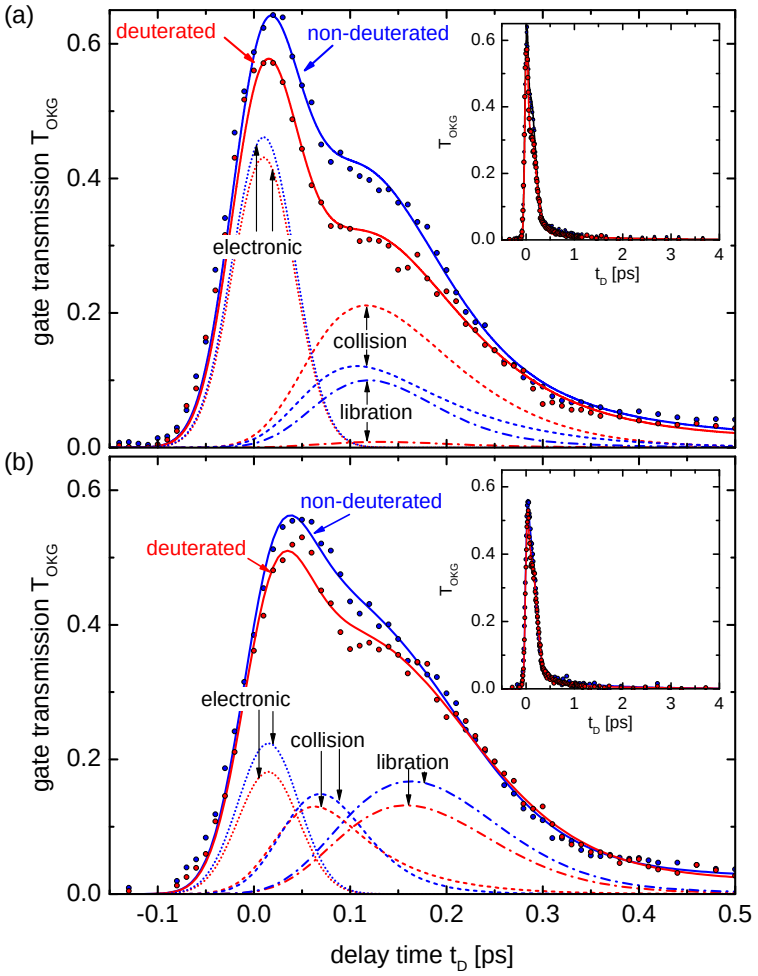

Fig. 3. Temporal distribution of the transmission of the OKG for (a) toluene and (b) nitrobenzene. The blue lines and dots refer to the non-deuterated liquids, the red to the corresponding deuterated substance. The insets show the time response up to 4 ps. Circles: measured data (circles), solid lines: fit to data points using Eq. (2) (parameters c.f. Table 3), dotted lines: electronic component, dashed lines: collision component, dashed-dotted lines: libration.

distortion might differ strongly between the investigated molecules due to their very different structure. Hence, more theoretical investigations of both molecule systems are necessary in order to explain the impact of collision more quantitatively. The increase of the time constant can be rationalized by inertia related slower molecular motion of the heavier deuterated specimen.

The libration related change of the nonlinear refractive index originates from a coherent rocking motion of aligned molecules. Dephasing e.g. due to collisions reduces this effect [22].

The time range of the collisonal interaction is comparable to that of the libration in case of toluene (between 0 fs and 300 fs). Thus, the dephasing based reduction of the libration might be very efficient in the presence of stronger collisions, particularly as only weak intermolecular interactions (e.g. van-der-Waals bondings [36]) should be present in the toluene matrix.

For nitrobenzene on the other hand the collisional interaction happens before the libration and thus the dephasing influence should be weaker. A possible reduction of the hydrogen bridging

Optics EXPRESS

strength to the exposed NO_2 group after deuteration might reduce the libration effect additionally [37].

An important issue that needs to be addressed is that the larger mass of deuterated molecules might affect the libration frequency characterized by ω_0 and σ (c.f. Table 1). The relative increase of the molecular mass due to deuteration amounts to 4 % for nitrobenzene and 8 % for toluene which is insignificant as the reduction of ω_0 below 10 % would be expected if a harmonic oscillator model would be assumed. Therefore the mass-induced impact is below the accuracy of ω_0 and σ and thus it is not considered as significant mechanism for the change of the librational contribution.

For both solvents, the diffusion related component of the nonlinear refractive index decreases slightly whereas its rise and fall times are increasing (c.f. Table 3) in case of deuteration. Like for the collision time, these changes are attributed to larger moment of inertia of the deuterated compared to the non-deuterated specimen. As compared to other relaxation channels the diffusive contribution only shows an insignificant differences between the original solvent signal and its deuterated counterpart. Therefore the individual contribution of the diffusion is not shown in Figs. 3(a) and 3(b) to retain the clarity of the figure.

Finally, it should be pointed out that a Raman related change of the nonlinear refracted index was observed neither for Nitrobenzene nor for Toluene and also not for the deuterated specimen. A higher temporal resolution of the OKG may be required to observe this effect.

The temporally integrated nonlinear refractive index variation of the deuterated compared to the non-deuterated specimen is calculated by the sum of the n_2 values (c.f. Table 3). This is of particular interest for fine-tuning the temporal response of nonlinear liquid-core devices in case pulses with durations of > 1 ps are considered. It reduces about 10 % in the case of Nitrobenzene (from $\Delta n_{ND} = (8.3 \pm 0.8) \cdot 10^{-19}$ m^2/W to $\Delta n_D = (7.6 \pm 0.8) \cdot 10^{-19}$ m^2/W and about 25 % for Toluene (from $\Delta n_{ND} = (4.3 \pm 0.3) \cdot 10^{-19}$ m^2 /W to $\Delta n_D = (3.5 \pm 0.3) \cdot 10^{-19}$ m^2/W).

7. Conclusion

Precise knowledge on the temporal response function of the incorporated materials is essential to understand nonlinear pulse propagation inside highly nonlinear media. Here we study the impact of deuteration onto the ultrafast dynamics of the nonlinear refractive index via all optical Kerr gating for two selected organic solvents, namely toluene and nitrobenzene. The resulting gate transmission functions of the deuterated specimen show different temporal evolutions compared to their non-deuterated counterparts, which was quantified by fitting the most recent mathematical model including the various physical phenomena to the measurement data.

We found that deuterated benzene derivates, which enable operation at near-infrared wavelength [24], overall show just slightly smaller nonlinearities than their non-deuterated counterparts (25 % for toluene and 10 % for nitrobenzene). These reduction is attributed to both, smaller electronic nonlinearities (i.e., smaller hyperpolarization) as well as weaker intermolecular interactions.

The results achieved are particularly relevant from the nonlinear device design perspective, e.g. for fine-tuning the nonlinear responses in magnitude and time by mixing different liquids [16]. For instance, tuning non-instantaneous effects can lead to nonlinear phase stabilization, which enables a suppression of noise-driven (spontaneous) parametric effects in supercontinuum generation in liquid-core fibers via controlling the strength of the delayed molecular nonlinearity [18,38]. Simulations that include the precise form of the nonlinear response function are the subject of a future publication.

Appendix: Transmission function of an optical Kerr gate

In the scope of the model it is assumed, that solely the pump pulse generates a nonlinear refractive index modification. The intensity of the probe pulse is considered to be weak. Furthermore

Optics EXPRESS

the sample medium is considered to be homogeneous. Hence the nonlinear refractive index is modelled by:

$$\Delta n(t) = \sum_m \alpha_m n_{2,m} r_m(t), \tag{3}$$

with α_m being a factor related to the polarization ellipsoid, $n_{2,m}$ the strength and $r_m(t)$ the time dependence of the component of the nonlinear refractive index. $r_m(t)$ was normalized such that $\int_{-\infty}^{+\infty} r_m(t)dt = 1$.

The refractive index modification after travelling through the medium of thickness d caused by the pump pulse leads to a spatially and temporally dependent phase delay of the probe pulse field component parallel to the pump field compared to the perpendicular one. This phase difference is described by:

$$\Delta\phi(t,r) = \frac{2\pi d}{\lambda_{pr}} \left(I_{pu}(t,r) \otimes \Delta n(t)\right) \tag{4}$$

Hence the transmitted energy for one delay time t_D is given by:

$$\begin{aligned} E_T(t_D) &= \pi \int_{-\infty}^{+\infty} \int_0^{+\infty} r I_{in}(r,t) \left(1 - \cos\left(\Delta\phi(r, t - t_D)\right)\right) dr dt \\ &= \pi \int_{-\infty}^{+\infty} \int_0^{+\infty} r I_{in}(r,t) \sum_{k=1}^{\infty} \frac{(-1)^{k-1}}{(2k)!} \left(\Delta\phi(r, t - d_D)\right)^{2k} dr dt \end{aligned} \tag{5}$$

Assuming Gaussian pulses in space and time the phase, the probe pulse intensity and the input probe pulse energy are:

$$\begin{aligned} \Delta\phi(t,r) &= \frac{2\pi d}{\lambda_{pr}} I_{0,pu} e^{-2\frac{r^2}{w_{pu}^2}} \left(e^{-4\ln 2 \frac{r^2}{\tau_{pu}^2}} \otimes \Delta n(t) \right) \\ I_{in}(r,t) &= I_{0,pr} e^{-2\frac{r^2}{w_{pr}^2}} e^{-4\ln 2 \frac{r^2}{\tau_{pr}^2}} \\ E_{in} &= \sqrt{\frac{\pi^3}{16\ln 2}} w_{pr}^2 \tau_{pr} I_{0,pr}, \end{aligned} \tag{6}$$

with $w_{pu,pr}$ being the $1/e^2$-radius, $\tau_{pu,pr}$ the FWHM pulse duration, and $I_{0,pu,pr}$ the peak intensity of the pump and the probe pulse, respectively.

Defining the transmission as $T_{OKG}(t_D) = E(t_D)/E_{in}$ and inserting (6) in (5) yields (1)

Funding

Deutsche Forschungsgemeinschaft (SCHM/2655/3-1, SCHM2655/10-1, SCHM2655/12-1); Thüringer Ministerium für Wirtschaft, Wissenschaft und Digitale Gesellschaft (Institutional funding).

Acknowledgments

We thank Dr. Wolfgang Paa, Prof. Wolfgang Triebel and Prof. Herbert Stafast for fruitful discussions regarding the optical Kerr gating technique.

Disclosures

The authors declare that there are no conflicts of interest related to this article.

Optics EXPRESS

References

1. T. Gottschall, T. Meyer, M. Baumgartl, C. Jauregui, M. Schmitt, J. Popp, J. Limpert, and A. Tünnermann, "Fiber-based light sources for biomedical applications of coherent anti-stokes raman scattering microscopy," Laser Photonics Rev. **9**(5), 435–451 (2015).
2. C. F. Kaminski, R. S. Watt, A. D. Elder, J. H. Frank, and J. Hult, "Supercontinuum radiation for applications in chemical sensing and microscopy," Appl. Phys. B: Lasers Opt. **92**(3), 367–378 (2008).
3. R. Slavik, F. Parmigiani, J. Kakande, C. Lundström, M. Sjödin, P. A. Andrekson, R. Weerasuriya, S. Sygletos, A. D. Ellis, L. Grüner-Nielsen, D. Jakobsen, S. Herstrøm, R. Phelan, J. O'Gorman, A. Bogris, D. Syvridis, S. Dasgupta, P. Petropoulos, and D. J. Richardson, "All-optical phase and amplitude regenerator for next-generation telecommunications systems," Nat. Photonics **4**(10), 690–695 (2010).
4. D. Blömer, A. Szameit, F. Dreisow, T. Schreiber, S. Nolte, and A. Tünnermann, "Nonlinear refractive index of fs-laser-written waveguides in fused silica," Opt. Express **14**(6), 2151–2157 (2006).
5. M. Grehn, T. Seuthe, W. Tsai, M. Höfner, A. W. Achtstein, A. Mermillod-Blondin, M. Eberstein, H. J. Eichler, and J. Bonse, "Nonlinear absorption and refraction of binary and ternary alkaline and alkaline earth silicate glasses," Opt. Mater. Express **3**(12), 2132–2140 (2013).
6. H. Hundertmark, S. Rammler, T. Wilken, R. Holzwarth, T. W. Hänsch, and P. S. Russell, "Octave-spanning supercontinuum generated in SF6-glass PCF by a 1060 nm mode-locked fibre laser delivering 20 pJ per pulse," Opt. Express **17**(3), 1919–1924 (2009).
7. X. Jiang, N. Y. Joly, M. A. Finger, F. Babic, G. K. L. Wong, J. C. Travers, and P. S. J. Russell, "Deep-ultraviolet to mid-infrared supercontinuum generated in solid-core ZBLAN photonic crystal fibre," Nat. Photonics **9**(2), 133–139 (2015).
8. D. D. Hudson, S. Antipov, L. Li, I. Alamgir, T. Hu, M. E. Amraoui, Y. Messaddeq, M. Rochette, S. D. Jackson, and A. Fuerbach, "Toward all-fiber supercontinuum spanning the mid-infrared," Optica **4**(10), 1163–1166 (2017).
9. K. F. Lee, N. Granzow, M. A. Schmidt, W. Chang, L. Wang, Q. Coulombier, J. Troles, N. Leindecker, K. L. Vodopyanov, P. G. Schunemann, M. E. Fermann, P. S. Russell, and I. Hartl, "Midinfrared frequency combs from coherent supercontinuum in chalcogenide and optical parametric oscillation," Opt. Lett. **39**(7), 2056–2059 (2014).
10. J. Ballato, H. Ebendorff-Heidepriem, J. Zhao, L. Petit, and J. Troles, "Glass and process development for the next generation of optical fibers: A review," Fibers **5**(1), 11 (2017).
11. M. Vieweg, T. Gissibl, S. Pricking, B. T. Kuhlmey, D. C. Wu, B. J. Eggleton, and H. Giessen, "Ultrafast nonlinear optofluidics in selectively liquid-filled photonic crystal fibers," Opt. Express **18**(24), 25232–25240 (2010).
12. R. V. J. Raja, A. Husakou, J. Hermann, and K. Porsezian, "Supercontinuum generation in liquid-filled photonic crystal fiber with slow nonlinear response," J. Opt. Soc. Am. B **27**(9), 1763–1768 (2010).
13. K. Kieu, L. Schneebeli, R. A. Norwood, and N. Peyghambarian, "Integrated liquid-core optical fibers for ultra-efficient nonlinear liquid photonics," Opt. Express **20**(7), 8148–8154 (2012).
14. M. Chemnitz, R. Scheibinger, C. Gaida, M. Gebhardt, F. Stutzki, S. Pumpe, J. Kobelke, A. Tünnermann, J. Limpert, and M. A. Schmidt, "Thermodynamic control of soliton dynamics in liquid-core fibers," Optica **5**(6), 695–703 (2018).
15. E. T. J. Nibbering, M. A. Franco, B. S. Prade, G. Grillon, C. L. Blanc, and A. Mysyrowicz, "Measurement of the nonlinear refractive index of transparent materials by spectral analysis after nonlinear propagation," Opt. Commun. **119**(5-6), 479–484 (1995).
16. P. Zhao, M. Reichert, B. Sepehr, D. J. Hagan, and E. W. van Stryland, "Temporal and polarization dependenceof the nonlinear optical response of solvents," Optica **5**(5), 583–594 (2018).
17. K. Iliopoulos, D. Potamianos, E. Kakkava, P. Aloukos, I. Orfanos, and S. Couris, "Ultrafast third order nonlinearities of organic solvents," Opt. Express **23**(19), 24171–24176 (2015).
18. M. Chemnitz, M. Gebhardt, C. Gaida, F. Stutzki, J. Kobelke, J. Limpert, A. Tunnermann, and M. A. Schmidt, "Hybrid soliton dynamics in liquid-core fibres," Nat. Commun. **8**(1), 42 (2017).
19. M. Reichert, H. Hu, M. R. Ferdinandus, M. Seidel, P. Zhao, T. R. Ensley, D. Peceli, J. M. Reed, D. A. Fishman, S. Webster, D. J. Hagan, and E. W. van Stryland, "Temporal, spectral, and polarization dependence of the nonlinear optical response of carbon disulfide: erratum," Optica **3**(6), 657–658 (2016).
20. D. J. Hagan, P. Zhao, M. Reichert, and E. W. van Stryland, "Comparison of second hyperpolarizability in liquid and gas phases of carbon disulfide," in *Advanced Photonics 2016 (IPR, NOMA, Sensors, Networks, SPPCom, SOF)*, (Optical Society of America, 2016), p. NoW2D.2.
21. K. Schaarschmidt, H. Xuan, I. H. J. Kobelke, M. Chemnitz, and M. A. Schmidt, "Long-term stable supercontinuum generation and watt-level transmission in liquid-core optical fibers," Opt. Lett. **44**(9), 2236–2239 (2019).
22. M. Reichert, H. Hu, M. R. Ferdinandus, M. Seidel, P. Zhao, T. R. Ensley, D. Peceli, J. M. Reed, D. A. Fishman, S. Webster, D. J. Hagan, and E. W. van Stryland, "Temporal, spectral, and polarization dependence of the nonlinear optical response of carbon disulfide," Optica **1**(6), 436–445 (2014).
23. R. A. Ganeev, A. I. Ryasnyansky, M. Baba, M. Suzuki, N. Ishizawa, M. Turu, S. Sakakibara, and H. Kuroda, "Nonlinear refraction in CS_2," Appl. Phys. B: Lasers Opt. **78**(3-4), 433–438 (2004).
24. M. Plidschun, M. Chemnitz, and M. A. Schmidt, "Low-loss deuterated organic solvents for visible and near-infrared photonics," Opt. Mater. Express **7**(4), 1122–1130 (2017).
25. S. Kedenburg, M. Vieweg, T. Gissibl, and H. Giessen, "Linear refractive index and absorption measurements of nonlinear optical liquids in the visible and near-infrared spectral region," Opt. Mater. Express **2**(11), 1588–1611 (2012).

Optics EXPRESS

26. D. McMorrow, N. Thantu, V. Kleiman, J. S. Melinger, and W. T. Lotshaw, "Analysis of intermolecular coordinate contributions to third-order ultrafast spectroscopy of liquids in the harmonic oscillator limit," J. Phys. Chem. A **105**(34), 7960–7972 (2001).
27. I. A. Heisler, R. R. Correia, T. Buckup, S. L. Cunha, and N. P. da Silveira, "Time-resolved optical Kerr-effect investigation on CS_2/polystyrene mixtures," J. Chem. Phys. **123**(5), 054509 (2005).
28. C. Kalpouzos, D. McMorrow, W. T. Lotshaw, and G. A. Kenney-Wallace, "Femtosecond laser-induced optical kerr dynamics in CS_2/alkane binary solutions," Chem. Phys. Lett. **150**(1-2), 138–146 (1988).
29. J. S. Friedman and C. Y. She, "The effects of molecular geometry on the depolarized stimulated gain spectra of simple liquids," J. Chem. Phys. **99**(7), 4960–4969 (1993).
30. R. W. Boyd, *Nonlinear Optic* (Academic, Amsterdam, 2008).
31. M. Ziólek, M. Lorenc, and R. Naskrecki, "Determination of the temporal response function in femtosecond pump-probe systems," Appl. Phys. B: Lasers Opt. **72**(7), 843–847 (2001).
32. R. Tammer and W. Hüttner, "The anisotropy of the second hyperpolarizability of molecular hydrogen from the pressure and temperature dependence of the Kerr effect," Chem. Phys. **146**(1-2), 155–163 (1990).
33. D. M. Bishop, J. Pipin, and M. Rérat, "Nonlinear optical properties of H2 and D2," J. Chem. Phys. **92**(3), 1902–1908 (1990).
34. Y. R. Luo, *Comprehensive Handbook of Chemical Bond Energies* (CRC, Boca Raton, 2007).
35. J. Bucaro and T. Litovitz, "Rayleigh scattering: Collisional motions in liquids," J. Chem. Phys. **54**(9), 3846–3853 (1971).
36. M. Schauer and E. Bernstein, "Calculations of the geometry and binding energy of aromatic dimers: Benzene, toluene, and toluene-benzene," J. Chem. Phys. **82**(8), 3722–3727 (1985).
37. S. Scheiner and M. Čuma, "Relative stability of hydrogen and deuterium bonds," J. Am. Chem. Soc. **118**(6), 1511–1521 (1996).
38. M. Chemnitz, C. Gaida, M. Gebhardt, F. Stutzki, J. Kobelke, A. Tunnermann, J. Limpert, and M. A. Schmidt, "Carbon chloride-core fibers for soliton mediated supercontinuum generation," Opt. Express **26**(3), 3221–3235 (2018).

194.95.159.93 (to 2020-01-03 07:44:54)